

Dissipative phase transition and metrology in collectively pumped superradiance

Yoav Shimshi and Ephraim Shahmoon

Department of Chemical & Biological Physics, Weizmann Institute of Science, Rehovot 7610001, Israel

(Dated: August 23, 2024)

We study a many-atom system exhibiting two competing collective processes: collective decay and collective pumping of excitations, relevant e.g. in cavity QED platforms. We find that the steady state exhibits a sharp transition as a function of the pumping strength, between fully depopulated and fully populated states. We devise a metrological protocol for measuring system parameters by scanning the pumping around the critical point, finding that the sensitivity scales as $1/N$, thus beating the standard quantum limit thanks to the buildup of correlations. Crucially, our theoretical analysis, verified numerically, goes beyond the adiabatic regime of an infinite scan time: we study non-equilibrium relaxation dynamics around the transition and their effect on the sensitivity, revealing that the favorable $1/N$ scaling survives well beyond adiabaticity. Apart from its direct impact on metrology with superradiant atomic systems, our general analysis provides new perspectives for studying the metrological utility of dissipative phase transitions in realistic finite-time protocols.

Recent progress in the study of driven-dissipative quantum systems has revealed new phenomena with potential applications in quantum technologies. In particular, the steady state of dissipative quantum systems may exhibit rich phases and entanglement properties [1–17], and can be exploited for novel approaches to quantum computing, simulation and state engineering [18–28]. Importantly, the existence of critical steady states that are arbitrarily sensitive to changes in external parameters opens the door to metrological protocols which are both insensitive to initial state preparation and robust to external noise [29–34]. This increased sensitivity is typically offset by critical slowing down of the relaxation rate near the transition, requiring prolonged protocol times to benefit from the sensitivity of the steady state [35–38].

In this work, we study a new dissipative phase transition and its application in metrology, while accounting for dynamical effects on sensitivity. We introduce a simple yet realistic model of a collective spin system in the context of superradiance. Superradiance describes the collective radiation of an ensemble of atom-like emitters to common field modes [39–42]; in its simplest form, it assumes a permutation symmetry between the atoms in their interaction with the field modes, as can be realized by trapping atoms inside an optical cavity. Steady state is reached when the atoms are constantly excited, forming a driven-dissipative system. When the drive is coherent the steady state is known to exhibit a second order phase transition at a critical drive strength [6, 13, 15, 43–51]. Incoherent excitation via individual optical pumping of each atom was also considered, with the prospect of designing ultranarrowband laser sources [52–56]. While the individual form of the optical pumping breaks the permutation symmetry between the atoms, the radiation is still collective and can exhibit a superradiant enhancement [57–59].

Here instead, we consider a situation where both the optical pumping and the dissipation are performed collectively. This results in a fully permutation symmetric model of a driven-dissipative system. We devise a quantum optical realization using an atomic ensemble coupled

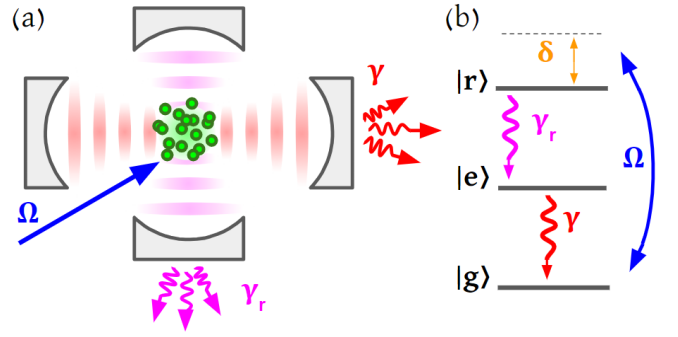


FIG. 1. Proposed realization of collectively pumped superradiance, Eq. (1). (a) An atomic ensemble coupled to two independent cavity modes (either of two distinct cavities or of the same cavity). The horizontal red mode mediates collective decay at rate γ while the vertical purple mode, together with external laser light (Rabi frequency Ω and detuning δ), generate collective pumping at a rate $w = \gamma_r(\Omega/\delta)^2$. (b) Level structure of each atom.

to two cavity modes (see Fig. 1) and analyze the steady state and dynamics. Due to the strong competition between collectively enhanced dissipation and pumping the steady state displays a sharp transition between fully populated and fully depleted states at a critical pumping value. We study this transition from the viewpoint of critical metrology, and show that under adiabatic conditions the sensitivity in estimating the critical pumping strength scales with the atom number N as $1/N$, thus beating the standard quantum limit [60–62]. Considering a realistic sensing protocol based on scanning the pumping parameters around the transition point, we develop a modified sensitivity estimate that accounts for non-adiabatic effects due to critical slowing down [37, 63, 64]. We find the scaling of the sensitivity with the scanning rate, and importantly show that the favorable $1/N$ scaling is maintained even beyond adiabatic conditions.

Model and realization.—We consider N two-level atoms undergoing collective dissipation and pumping, as described by the following master equation for the many-

atom density matrix $\hat{\rho}$,

$$\dot{\hat{\rho}} = \gamma \mathcal{D}_{\hat{J}_-}[\hat{\rho}] + w \mathcal{D}_{\hat{J}_+}[\hat{\rho}], \quad (1)$$

with $\mathcal{D}_{\hat{A}}[\hat{\rho}] \equiv \hat{A}\hat{\rho}\hat{A}^\dagger - \frac{1}{2}\{\hat{A}^\dagger\hat{A}, \hat{\rho}\}$ denoting the Lindblad-form irreversible process governed by a so-called jump operator \hat{A} . The first term, with jump operator $\hat{J}_- = \sum_{n=1}^N |g_n\rangle\langle e_n|$ ($|g_n\rangle$ and $|e_n\rangle$ denoting the ground and excited levels of atom n) accounts for collective radiation at rate γ , while the second term (with jump operator $\hat{J}_+ = \hat{J}_-^\dagger$) describes incoherent, collective pumping of the atoms at rate w . Notably, the dynamics of Eq. (1) conserve the total spin number j of the atomic pseudo-spins. Assuming an initial fully unpopulated state such that $j = N/2$, the dynamics are thus confined to the Hilbert space of $N + 1$ angular momentum states $|m\rangle$ with $m = -N/2, \dots, N/2$ (Dicke states [39–41]).

The realization of the purely collective dynamics of Eq. (1) requires that both the decay and the pumping processes exhibit permutation symmetry between atoms at relevant experimental time scales. Collective decay is commonly achieved by trapping the atoms inside a cavity such that they exhibit uniform coupling to the rapidly decaying cavity mode resonant with the $|g\rangle \leftrightarrow |e\rangle$ transition, resulting in collective radiation at the cavity-enhanced rate γ (Fig. 1a) [40, 52]. Meanwhile, optical pumping requires considering a third level $|r\rangle$ coherently coupled to $|g\rangle$ by laser light (Rabi frequency Ω and detuning δ), from which excitations decay to $|e\rangle$ at a rate γ_r , thus completing an incoherent excitation from $|g\rangle$ to $|e\rangle$. While the latter $|r\rangle \rightarrow |e\rangle$ decay is typically taken to be individual, thereby leading to individual pumping, we now present a scheme that instead leads to collective pumping. Specifically, we consider an additional cavity mode (either a different longitudinal mode in the same cavity or a different cavity (see Fig. 1a and Appendix A), this time resonant with the $|e\rangle \leftrightarrow |r\rangle$ transition, to which the atoms are also coupled uniformly. Adiabatically eliminating both of the fast-decaying cavity modes, we arrive at the master equation for the density matrix \hat{R} of the N 3-level atoms,

$$\begin{aligned} \dot{\hat{R}} = & -i \left[-\delta \hat{J}_{rr} + \Omega \left(\hat{J}_{rg} + \hat{J}_{gr} \right), \hat{R} \right] \\ & + \gamma \mathcal{D}_{\hat{J}_{ge}}[\hat{R}] + \gamma_r \mathcal{D}_{\hat{J}_{er}}[\hat{R}], \end{aligned} \quad (2)$$

with the atomic collective operators given by $\hat{J}_{\mu\nu} = \sum_{n=1}^N |\mu_n\rangle\langle \nu_n|$ for states $\mu, \nu \in \{g, e, r\}$.

In order to obtain an effective pumping from $|g\rangle$ to $|e\rangle$ we consider the situation where the $|r\rangle$ level is mostly depopulated due to a large detuning δ . Relevant collective states containing $|r\rangle$ are then restricted to the subspace containing only single $|r\rangle$ excitations, which is adiabatically eliminated by the self-consistent assumption of a detuning much larger than all other relevant rates ($\delta \gg \sqrt{N}\Omega, N\gamma_r, N^2\gamma$). This leads to an effective pumping within the reduced subspace of collective states containing only $|g\rangle$ and $|e\rangle$ as described by Eq. (1), yielding the pumping rate $w = (\Omega/\delta)^2\gamma_r$ given by the product

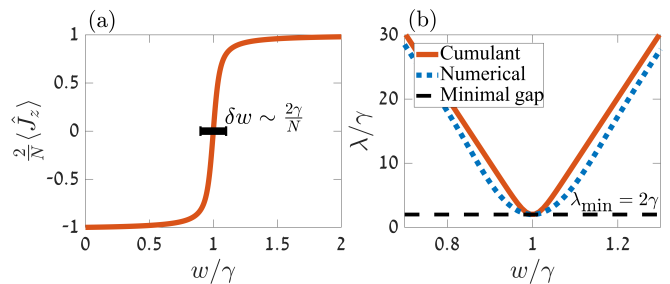


FIG. 2. (a) The mean population inversion in steady state, $\langle \hat{J}_z \rangle$ from Eq. (4), as a function of pumping rate w exhibits a sharp transition from depopulated to populated state at the critical value $w = \gamma$. (b) Relaxation rate λ as a function of pumping w . Good agreement between analytical cumulant-expansion results of Eq. (7) (solid red) and numerical calculation of Liouville gap of Eq. (1) (dotted blue) is observed, yielding a finite minimal gap $\lambda_{\min} = 2\gamma$ at the critical point $w = \gamma$ (dashed black). $N = 100$ atoms is taken in all plots.

of collective- $|r\rangle$ -state population and their decay rate γ_r , and with $\hat{J}_- = \hat{J}_{ge}$. Our full derivation of Eq. (1) starting from Eq. (2) is presented in Appendix B, utilizing the generalized adiabatic elimination formulation of [23].

Steady state solution.—Looking at Eq. (1), we note that the pumping term is mathematically analogous to the effect of heat flowing into the system from a finite temperature reservoir. In particular, we identify an effective ‘temperature’ $\beta \equiv -\ln(w/\gamma)$, thus anticipating that the steady state would be equivalent to thermal Boltzmann statistics. Indeed, we find that Eq. (1) has the unique steady state (Appendix C)

$$\hat{\rho}_s = \frac{1}{Z(\beta)} e^{-\beta \hat{J}_z}, \quad Z(\beta) = \frac{\sinh((N+1)\beta/2)}{\sinh(\beta/2)}, \quad (3)$$

with the population inversion operator $\hat{J}_z = (\hat{J}_{ee} - \hat{J}_{gg})/2$ taking the role of ‘energy’. We can easily derive exact expressions for moments of \hat{J}_z using the partition function, such as $\langle \hat{J}_z \rangle = -\partial_\beta \ln Z(\beta)$. For $N \gg 1$ and $|w/\gamma - 1| \ll 1$ we obtain

$$\begin{aligned} \langle \hat{J}_z \rangle = & \frac{N/2}{\tanh(N(w/\gamma - 1)/2)} - \frac{1}{w/\gamma - 1} \\ N \xrightarrow{\rightarrow} \infty & \begin{cases} \frac{N}{2} \text{sign}(w/\gamma - 1) & |w/\gamma - 1| \gg \frac{1}{N} \\ \frac{N^2}{12} (w/\gamma - 1) & |w/\gamma - 1| \ll \frac{1}{N} \end{cases}. \end{aligned} \quad (4)$$

At the ‘thermodynamic limit’, $N \rightarrow \infty$, the system exhibits a sharp jump at a critical pumping rate $w = \gamma$ from a fully depleted ($w < \gamma$) to a fully populated state ($w > \gamma$), as clearly seen in the exact solution plotted in Fig. 2a. This abrupt switching between the two states originates in the nonlinear pull from the competing dissipation and pumping processes in Eq. (1), which are exactly balanced at the transition point $w = \gamma$. The width of the transition region is of order $2\gamma/N$, shrinking to zero as $N \rightarrow \infty$.

Metrological application.—Evidently, near the transition measurements of the mean population are highly sensitive to changes in the pumping rate w . One might then imagine a procedure where w is scanned adiabatically and we locate the critical rate $w = \gamma$ at which the population jumps to an accuracy of $\delta w \sim 2\gamma/N$. This can be achieved by monitoring off-cavity-axis fluorescence, which is proportional to the mean excited atom population. The sensitivity in measuring $w/\gamma = (\Omega/\delta)^2 (\gamma_r/\gamma)$ can then be exploited for precise estimation of system parameters (e.g. γ , γ_r , δ , Ω) or external fields that determine their value. Extracted from population measurements around the transition $w = \gamma$ (where $\beta \approx 1 - w/\gamma$), this sensitivity is then given by the rate of change of $\langle \hat{J}_z \rangle$ and by the strength of fluctuations $\text{Var}[\hat{J}_z] = \partial_\beta^2 \ln Z(\beta) = -\partial_\beta \langle \hat{J}_z \rangle$, as per the error propagation formula, obtaining

$$\delta w \approx \gamma \frac{\sqrt{\text{Var}[\hat{J}_z]}}{|\partial_\beta \langle \hat{J}_z \rangle|} = \frac{\sqrt{12}\gamma}{N}. \quad (5)$$

This result shows that the sensitivity in w (or quantities that determine it) scales like $1/N$, suggesting enhanced sensitivity that far exceeds the scaling $1/\sqrt{N}$ of statistically independent atoms. This enhancement originates in correlations between atoms generated by the collective character of dissipation and pumping. Importantly, the sensitivity achieved in Eq. (5) is in fact the optimal one; we show this by calculating the Fisher information, verifying that (5) saturates the Cramér-Rau bound (Appendix D)[65].

While the result (5) implies excellent scaling of the sensitivity, we recall that its strict validity requires that the system remains in steady-state throughout the scan of pumping values w around the critical point. However, close to a phase transition one typically expects critical slowing down of the relaxation time, imposing increasingly slower scanning rates of w to adiabatically remain in steady state. This limits the number of scans we can take, as the total experiment time is ultimately bounded by the individual emission time T of the atoms to off-cavity-axis modes, that breaks the purely collective physics described by Eq. (1).

To estimate the bounds under which the adiabatic assumption is valid we must calculate the system relaxation rate λ as a function of w . This can be done using the two-time correlation function $C_{zz}(\tau) = \langle \hat{J}_z(t + \tau) \hat{J}_z(t) \rangle - \langle \hat{J}_z(t + \tau) \rangle \langle \hat{J}_z(t) \rangle$, which exhibits approximate exponential scaling $e^{-\lambda\tau}$ at long times. Using the quantum regression theorem [66] and neglecting third order cumulants [67] we derive (Appendix E),

$$\partial_\tau C_{zz}(\tau) \approx -\lambda(w) C_{zz}(\tau), \quad (6)$$

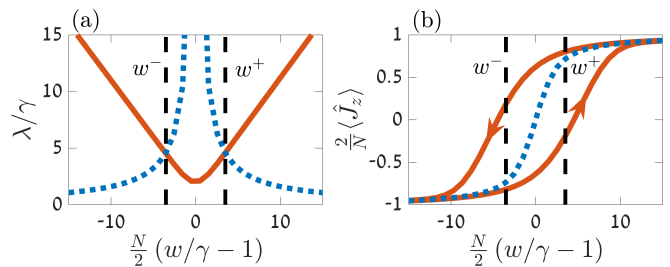


FIG. 3. (a) Relaxation rate λ (solid red) and normalized scanning rate $\dot{w}/|w - \gamma| \propto 1/|w - \gamma|$ of the pumping strength w (dashed blue) as a function of w , for constant scanning rate $r \equiv \dot{w} \frac{N}{2\gamma} = 16\gamma$ and $N = 100$. Dashed horizontal lines mark the boundaries w^\pm within which the scanning rate is too fast for the system to adiabatically follow the steady state solution. (b) A hysteresis loop of the mean inversion $\langle \hat{J}_z \rangle$ (solid red) is formed around the steady state solution (4) (dashed blue) due to the dynamics induced by the scanning rate from (a). The horizontal lines approximately bound the region of freezing and thawing of the dynamics as deduced from (a).

with the relaxation rate given by

$$\lambda(w) = \frac{N(w - \gamma)}{\tanh(N/2(w/\gamma - 1))} \quad (7)$$

$$\approx \begin{cases} N|w - \gamma| & |w/\gamma - 1| \gg \frac{1}{N} \\ 2\gamma & |w/\gamma - 1| \ll \frac{1}{N} \end{cases}.$$

In Fig. 2b we plot the rate from Eq. (7), compared to that obtained by a numerical calculation of the lowest non-vanishing eigenvalue (Liouville gap) of the rate equation for populations $\langle m | \hat{\rho} | m \rangle$ obtained from Eq. (1) (Appendices C,E). Very good agreement is observed for relevant regions $|w/\gamma - 1| \ll \frac{1}{N}$ and $|w/\gamma - 1| \gg \frac{1}{N}$, and a decrease of the relaxation rate ('slowing down') around the critical point is indeed observed.

Interestingly, we observe that the minimal gap (rate) obtained at the critical point has a finite value, $\lambda_{\min} = 2\gamma$, even at the thermodynamic limit $N \rightarrow \infty$. This means that the system always reaches steady state at a finite time, ensuring the possibility for adiabatic conditions and hence the favorable $1/N$ sensitivity scaling from (5) at any system size. This is in stark contrast to typical critical systems wherein the gap tends to zero as $N \rightarrow \infty$ [1].

Dynamical effects.—While the gap is always finite, it might still be very small in some particular realizations, motivating us to study the behavior of the system outside of adiabatic conditions. Remarkably, we find that even beyond adiabaticity, the favorable $1/N$ scaling in sensitivity still holds. To see this, we consider a scenario in which the pumping changes at a constant rate $\dot{w} = \frac{2\gamma}{N}r$ ($1/r$ being the scan time of the transition width $\sim \frac{2\gamma}{N}$). The scanning rate is then characterized by the natural timescale $\dot{w}/|w - \gamma|$, exhibiting a hyperbolic shape $\propto 1/|w - \gamma|$ for our constant \dot{w} . In the region $\dot{w}/|w - \gamma| \geq \lambda(w)$ the scanning timescale is faster than

that of relaxation (Fig. 3a), and consequently the population does not follow steady state behavior. Instead it 'freezes' in the value it had in entering the non-adiabatic region, and only 'thaws out' when the pumping parameter leaves the region (Fig. 3). This process repeats if the pumping is varied in the opposite direction, only with the points of freezing and thawing switching roles. Thus upon periodic variation of w around the transition point the population traces a hysteresis loop (Fig. 3b).

The solution for the boundaries of the adiabatic region $\dot{w}/|w - \gamma| = \lambda(w)$, with λ from (7) and using $\dot{w} = \frac{2\gamma}{N}r$, yields the points $w^\pm(r)$ of freezing and thawing, and hence an estimate for the hysteresis width $\Delta w_H(r) \equiv |w^+(r) - w^-(r)|$ (Fig. 3),

$$\Delta w_H(r) \approx \frac{2\gamma}{N} \times \begin{cases} r/\gamma & r \ll \gamma \\ \sqrt{2r/\gamma} & r \gg \gamma \end{cases}. \quad (8)$$

Considering first the case of slow scanning, $r \ll \gamma$, we observe that the loop's width scales linearly with r , and the hysteresis width is much smaller than the steady state transition width $2\gamma/N$. This means that the hysteretic behavior is negligible and the sensitivity in estimation of w is given by Eq. (5). When $r \gg \gamma$ the loop becomes wider than the transition width and grows as $\sqrt{r/\gamma}$. At this point the transition width is no longer relevant for estimating the sensitivity, and all we can say for sure is that the 'true' transition is inside a region of width Δw_H . The 'corrected' sensitivity per single independent run of the experiment is then estimated as $\delta w \sim \max\{\frac{\sqrt{12}\gamma}{N}, \Delta w_H\}$.

Numerical simulation.—The prediction of Eq. (8) can be checked against results obtained from direct numerical simulation of Eq. (1) with the time-dependent pumping $w(t) = 2\gamma r t/N$. Plotting $\langle \hat{J}_z(t) \rangle$ as a function of $w(t)$ for positive and negative r gives us a hysteresis loop, as shown in Fig. 3b for $r = 16\gamma$ and $N = 100$. The width $\Delta w_H(r)$ is then calculated numerically by extracting the crossing points of the loop with the $\langle \hat{J}_z \rangle = 0$ axis. Running the procedure for different values of r then allows us to obtain Δw_H as a function of r as plotted in Fig. 4a.

For slow scanning rates, $r \ll \gamma$, we observe an excellent agreement with the linear dependence predicted in Eq. (8). For faster rates, $r \gg \gamma$, the fit to a power-law yields $\Delta w_H \propto (r/\gamma)^\eta$ with $\eta \approx 0.6$, fairly close to the $\eta = 0.5$ prediction of Eq. (8). The slight deviation in η is attributed to the existence of additional timescales in the long-time behavior of Eq. (1), which perturb the relaxation dynamics from the assumed purely exponential decay at a single rate λ (see Appendix F). Moreover, comparing the different $\Delta w_H(r)$ curves obtained for different values of N and scaled to $2\gamma/N$, we verify in Fig. 4b that they all collapse on each other in accordance with the prediction of Eq. (8) wherein $(N/2\gamma)\Delta w_H$ is independent of N .

Total sensitivity.—Intuitively, our estimation of the hysteresis width tells us that we can preform our measurement adiabatically as long as $r \lesssim \gamma$, yielding a single-scan sensitivity of order $\sim 2\gamma/N$. Then, for a total exper-

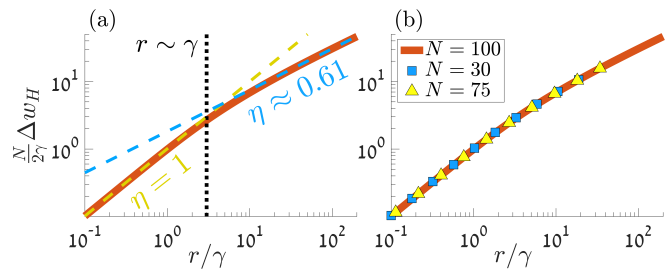


FIG. 4. Hysteresis width Δw_H (scaled to $2\gamma/N$) vs. scanning rate r , obtained numerically (see text). (a) For $N = 100$. Dashed asymptotes indicate power-law behavior, switching from a power $\eta = 1$ to a power $\eta \approx 0.61$ around a critical scanning rate $r \sim \gamma$, similar to the prediction of Eq. (8). Slight deviation from the $\eta = 0.5$ prediction for $r > \gamma$ is originated in the existence of multiple timescales (see Appendix F). (b) The different curves of Δw_H (scaled to $2\gamma/N$) obtained for different N values are seen to collapse on each other in accordance with the prediction of Eq. (8).

iment time T set by the timescale of competing individual decay processes, a rate of $r \sim \gamma$ yields the maximum number of independent scans close to adiabaticity, thus improving the overall sensitivity beyond that of a single scan $\sim 2\gamma/N$ by an additional factor $\sim 1/\sqrt{\gamma T}$. This intuitive argument can be made more accurate as follows.

According to Fig. 4a, the widening of the hysteresis leads to an increase in the uncertainty for estimating the transition point, which scales as $(r/\gamma)^\eta$, thus favoring a small scan rate r . However, a faster rate of scanning allows to preform more independent scans within a given experiment time T , leading to lower total uncertainty. To capture this trade-off we estimate the number of independent scans attainable at a rate r . First, the range of pump values covered by each independent scan should be large enough to capture the whole transition, setting it to $\Delta w_{\text{scan}} = C\delta w \sim \frac{\gamma C}{N} \times \max\{1, (r/\gamma)^\eta\}$, with a dimensionless constant $C > 1$. Then, in a total experiment time T , one can preform $N_s = \dot{w}T/2\Delta w_{\text{scan}}$ independent scans. This yields the estimate for the total sensitivity in our measurement as

$$\delta w_{\text{total}} \approx \frac{\delta w}{\sqrt{N_s}} \sim \frac{\gamma}{N} \sqrt{\frac{C}{\gamma T}} \times \begin{cases} (r/\gamma)^{-1/2} & r \ll \gamma \\ (r/\gamma)^{\frac{3\eta-1}{2}} & r \gg \gamma \end{cases}, \quad (9)$$

where here $\eta \sim 0.6$ is the numerically found power-law from Fig 4a. Unlike Eq. (5), this expression takes into account the number of repetitions possible before the experiment time ends. It also depends on the pumping range chosen for each scan, which we have set to vary with r to accommodate the growing hysteresis loop. Remarkably, our result shows that even well above the optimal adiabatic rate $r \sim \gamma$ the sensitivity retains its $1/N$ scaling, with a moderate widening factor $\sim (r/\gamma)^{0.4}$.

Discussion.—In summary, we have shown that collectively pumped superradiant emitters can be used as a platform for quantum critical metrology, and that favorable scaling of the sensitivity with atom number can be

achieved when the system is scanned at a rate both below the adiabatic region and above it. The system we analyzed can be readily implemented in cavity QED settings where great control over atomic positions is possible (for example in optical lattices [55, 68, 69] or using optical tweezers [70]). Our analysis of the scanning protocol and relaxation rates relying on a first order phase transition opens the path for further exploration of time-dependence in dissipative phase transitions beyond adiabaticity. In particular, an important direction would be the detailed analysis of the scaling of parameters that characterize the width and shape of the hysteresis loop, and how such information could be exploited for improved metrological capabilities.

ACKNOWLEDGMENTS

We acknowledge financial support from the Israel Science Foundation (ISF), the ISF and the Directorate for Defense Research and Development (DDR&D), the Center for New Scientists at the Weizmann Institute of Science, the Council for Higher Education (Israel). This research is made possible in part by the historic generosity of the Harold Perlman Family.

Appendix A: Realization of cavity mode coupling

In the paper we suggested implementing both collective dissipation and pumping in an atomic ensemble by using two independent cavity modes to which the all the atoms are coupled in an identical way. While in Fig. 1 of the main text we depict, for conceptual simplicity, the possibility to use two distinct cavities to this end, here we describe how a single cavity can suffice. To see this, assume that we are working in the Rayleigh range and that many wavelengths fit within it. Consider two longitudinal cavity modes \hat{a} and \hat{b} , resonant with the $|e\rangle \leftrightarrow |g\rangle$ transition and the $|r\rangle \leftrightarrow |e\rangle$ transition respectively. Identical coupling to the mode \hat{a} can be achieved if we place the atoms periodically along the cavity axis at a lattice distance $\lambda_a = 2\pi c/\omega_{ge}$ from each other (with ω_{ge} the relevant transition frequency) such that the atoms are sitting at the maxima of the mode's field strength. Meanwhile to attain identical coupling with \hat{b} we need to place the atoms a distance $\lambda_b = 2\pi c/\omega_{er}$ from each other, which is generally incompatible with the first restriction.

However, if the first condition is satisfied then there is a sufficiently large region along the atomic 'chain' where the mode shape of \hat{a} overlaps well with the mode shape of \hat{b} . Specifically, we assume the atoms are trapped at the antinodes of mode \hat{a} and within a total range of $\lambda_a \ll \Delta x \ll 2\pi/|k_a - k_b|$ which is much smaller than the difference of wavenumbers k_a and k_b of the two cavity modes (with $k_i = 2\pi/\lambda_i$). This can be done e.g. with a 1D optical lattice [55] or tweezer array [70], noting that such arrangement can fit multiple trapping

sites and atoms thanks to the length scale separation $|k_a - k_b| \ll 2\pi/\lambda_a$. Then, within Δx , both k_a and k_b appear almost identical, meaning that the atoms are approximately placed at the antinodes of both cavity modes simultaneously, so that they exhibit permutation symmetric coupling to both cavity modes to an excellent degree.

Appendix B: Derivation of master equation (1)

Beginning with the master equation (2) in the main text, the derivation of the master equation (1) of collectively pumped superradiance must involve the adiabatic elimination of all the states that include atoms excited to the state $|r\rangle$. In the following, we first present the full derivation, based on a generalized formulation of adiabatic elimination of open systems (subsections B 1 and B 2) and then consider an alternative, intuitive approach (subsection B 3).

1. Generalized adiabatic elimination method

In order to derive the master equation presented in the main text's Eq. (1), we used an adiabatic elimination scheme first described by [23]. We will present it in a form suited for use in our case.

We start with a system comprised of two sub-spaces, a ground Hilbert space \mathcal{H}_G and an excited Hilbert space \mathcal{H}_E . We want to look at a situation where the state is with high probability in \mathcal{H}_G , and we weakly excite it into the fast evolving \mathcal{H}_E . We include a strong dissipation channel from the excited to the ground manifold such that all excitations decay fast to the ground and an effective description inside the ground manifold only is possible. We also introduce a slight modification to the formalism by adding a weak dissipation channel which doesn't mix between the two sub-spaces (this is relevant to our case, where collective decay from e to g is assumed). Assuming Markovian dynamics, the master equation for the state \hat{R} (defined on the total Hilbert space) can be expressed in Lindblad form as

$$\dot{\hat{R}} = -i \left[\hat{H} + \hat{V}, \hat{R} \right] + \mathcal{D}_{\hat{K}}[\hat{R}] + \mathcal{D}_{\hat{L}}[\hat{R}], \quad (\text{B1})$$

where \hat{H} is the Hamiltonian for the excited states, \hat{V} is the exciting perturbation, \hat{K} is the jump operator from the excited to the ground manifold and \hat{L} is the in-manifold jump. The formalism can be generalized straightforwardly by adding modifications such as slow ground evolution, a time dependent perturbation or multiple dissipation channels. However, for our purposes the formalism presented is enough. Our goal is to write the out-of-ground-manifold components of the density matrix in terms of the ground component, and to write an effective equation for the ground component. To this end

we decompose the density matrix, and likewise the different operators defining the state evolution, in a block form:

$$\hat{R} = \begin{pmatrix} \hat{\rho}_{EE} & \hat{\rho}_{EG} \\ \hat{\rho}_{GE} & \hat{\rho}_{GG} \end{pmatrix}, \quad (\text{B2})$$

$$\hat{H} = \begin{pmatrix} \hat{H}_{EE} & 0 \\ 0 & 0 \end{pmatrix}, \quad \hat{V} = \begin{pmatrix} 0 & \hat{V}_{EG} \\ \hat{V}_{GE} & 0 \end{pmatrix}, \quad (\text{B3})$$

$$\hat{K} = \begin{pmatrix} 0 & 0 \\ \hat{K}_{GE} & 0 \end{pmatrix}, \quad \hat{L} = \begin{pmatrix} \hat{L}_{EE} & 0 \\ 0 & \hat{L}_{GG} \end{pmatrix}.$$

Following [23], we can then write an effective evolution equation for the ground components

$$\dot{\hat{\rho}}_{GG} = -i \left[\hat{H}_{\text{eff}}, \hat{\rho}_{GG} \right] + \mathcal{D}_{L_{GG}}[\hat{\rho}_{GG}] + \mathcal{D}_{\hat{K}_{\text{eff}}}[\hat{\rho}_{GG}], \quad (\text{B4})$$

where

$$\hat{H}_{\text{eff}} = -\hat{V}_{GE} \frac{\hat{H}_{\text{nh}}^{-1} + \left(\hat{H}_{\text{nh}}^{-1} \right)^\dagger}{2} \hat{V}_{EG}, \quad (\text{B5})$$

$$\hat{K}_{\text{eff}} = -\hat{K}_{GE} \hat{H}_{\text{nh}}^{-1} \hat{V}_{EG}, \quad (\text{B6})$$

and where we define a non-Hermitian Hamiltonian \hat{H}_{nh} , which controls the dissipative evolution in the excited manifold

$$\hat{H}_{\text{nh}} = \hat{H}_{EE} - \frac{i}{2} \hat{K}_{EG} \hat{K}_{GE}. \quad (\text{B7})$$

Eq. (B4) is a valid approximation as long as the excited manifold is nearly depopulated. This holds when $\|\hat{H}_{\text{nh}}\| \gg \|\hat{V}_{GE}\|$ (where $\|\cdot\|$ is any matrix norm of your choosing, for example the spectral norm). We also note that our expression is slightly modified with respect to the one appearing in [23], due to the fact that we include in-manifold dissipation. This does not affect the pumping process as long as the rates given by \hat{L} are much lower than the rate of evolution in the excited manifold (this is enforced if $\|\hat{H}_{\text{nh}}\| \gg \|\hat{L}_{EE}\|, \|\hat{L}_{GG}\|$).

2. Application to the case of N three level atoms

Working with the atomic system as described in the paper (with mode coupling as described above), we can describe the dynamics of the atom using Eq. (2) in the main text:

$$\begin{aligned} \dot{\hat{R}} = & -i \left[-\delta \hat{J}_{rr} + \Omega \left(\hat{J}_{rg} + \hat{J}_{gr} \right), \hat{R} \right] \\ & + \gamma \mathcal{D}_{\hat{J}_{ge}}[\hat{R}] + \gamma_r \mathcal{D}_{\hat{J}_{er}}[\hat{R}]. \end{aligned} \quad (\text{B8})$$

Physically the state is mostly in the Dicke sector made up of e and g states, while a small percentage (of $O(N\Omega^2/\delta^2)$) have a single atom excited to the r level (there may be further excitations, but their occupation is

of $O\left((N\Omega^2/\delta^2)^2\right)$ and can therefore be neglected). This motivates us to define ground and excited manifolds as above:

$$\mathcal{H}_G = \text{span} \left\{ |m\rangle \equiv \left| \frac{N}{2}, m \right\rangle_{eg} \right\}_{m=-N/2}^{N/2}, \quad (\text{B9})$$

$$\begin{aligned} \mathcal{H}_E &= \hat{J}_{rg} \mathcal{H}_G \\ &= \text{span} \left\{ |m^+\rangle \equiv \frac{1}{\sqrt{N/2-m}} \hat{J}_{rg} \left| \frac{N}{2}, m \right\rangle_{eg} \right\}_{m=-N/2}^{N/2-1}. \end{aligned}$$

It is now straightforward to calculate the matrix elements of the various operators in Eq. (B8) needed to apply the formalism

$$\langle m^+ | \hat{H}_{EE} | n^+ \rangle = |n^+\rangle = -\delta \cdot \delta_{mn}, \quad (\text{B10})$$

$$\langle m^+ | \hat{V}_{EG} | n \rangle = \langle m^+ | \Omega \hat{J}_{rg} | n \rangle = \Omega \sqrt{\frac{N}{2} - m} \cdot \delta_{mn},$$

$$\begin{aligned} \langle m | \hat{L}_{GG} | n \rangle &= \langle m | \sqrt{\gamma} \hat{J}_{ge} | n \rangle \\ &= \delta_{m+1,n} \sqrt{\gamma \left(\frac{N}{2} - n + 1 \right) \left(\frac{N}{2} + n \right)}, \end{aligned}$$

$$\begin{aligned} \langle m | \hat{K}_{GE} | n^+ \rangle &= \langle m | \sqrt{\gamma_r} \hat{J}_{er} | n^+ \rangle \\ &= \delta_{m-1,n} \sqrt{\gamma_r \left(\frac{N}{2} + n + 1 \right)}, \end{aligned}$$

and similarly straightforward to calculate the effective Hamiltonian and jump operator resulting from the adiabatic elimination process

$$\langle m | \hat{K}_{\text{eff}} | n^+ \rangle = -\langle m | \hat{K}_{GE} \hat{H}_{\text{nh}}^{-1} \hat{V}_{EG} | n^+ \rangle \quad (\text{B11})$$

$$= \frac{\Omega \sqrt{\gamma_r \left(\frac{N}{2} - n \right) \left(\frac{N}{2} + n + 1 \right)}}{\delta \left(1 + \frac{i\gamma_r}{2\delta} \left(\frac{N}{2} + n + 1 \right) \right)} \delta_{m-1,n},$$

$$\begin{aligned} \langle m | \hat{H}_{\text{eff}} | n \rangle &= -\langle m | \hat{V}_{GE} \frac{\hat{H}_{\text{nh}}^{-1} + \left(\hat{H}_{\text{nh}}^{-1} \right)^\dagger}{2} \hat{V}_{EG} | n \rangle \\ &= \frac{\Omega^2}{\delta} \cdot \frac{\frac{N}{2} - m}{1 + \frac{\gamma_r^2}{4\delta^2} \left(\frac{N}{2} + m + 1 \right)^2} \delta_{mn}. \end{aligned} \quad (\text{B12})$$

In the high detuning limit $\delta \gg N\gamma_r$, these expressions simplify to $\hat{K}_{\text{eff}} = \frac{\Omega}{\delta} \sqrt{\gamma_r} \hat{J}_+$ and $\hat{H}_{\text{eff}} = \frac{\Omega^2}{\delta} \left(N - \hat{J}_z \right)$, and since the Hamiltonian term amounts to a simple energy shift we can eliminate it by moving to the appropriate rotating frame. The resulting ground state evolution is then

$$\dot{\hat{\rho}} = \mathcal{L}[\hat{\rho}] = \gamma \mathcal{D}_{\hat{J}_-}[\hat{\rho}] + w \mathcal{D}_{\hat{J}_+}[\hat{\rho}], \quad (\text{B13})$$

with $w = \gamma_r (\Omega/\delta)^2$, as in the main text. In addition, applying the conditions $\|\hat{H}_{\text{nh}}\| \gg \|\hat{V}_{GE}\|, \|\hat{L}_{EE}\|, \|\hat{L}_{GG}\|$ gives us the range of validity of our model, namely

$$N\gamma \ll \gamma_r \ll \frac{\delta}{N}. \quad (\text{B14})$$

3. Intuitive approach

Starting from Eq. (2) of the main text, the essence of the derivation is to obtain an incoherent term that couples the state $|m\rangle$ to the state $|m+1\rangle$ in the subspace of $\{g, e\}$ states. To this end, consider the state $|m, 0\rangle \equiv |m\rangle$, and the minimal process that can couple it to $|m+1, 0\rangle \equiv |m+1\rangle$ (in a perturbation theory sense, for weak drive Ω). First, the term $\Omega \hat{J}_{rg}$ coupled $|m\rangle$ to the state $|m, 1\rangle \equiv |m^+\rangle \propto \hat{J}_{rg} |m\rangle$, and then the latter state decays to $|m+1, 0\rangle$ via the collective dissipation term $\gamma_r \mathcal{D}_{\hat{j}_{er}}[\hat{R}]$. In addition, $|m+1, 0\rangle$ may decay to $|m, 0\rangle$ via the other collective dissipation term $\gamma \mathcal{D}_{\hat{j}_{ge}}[\hat{R}]$. The coupling and dissipation that gives rise to this process are summarized in Fig. 5. The different rates marked on the figure are obtained as follows:

- Drive $\Omega\sqrt{N/2 - m}$: The drive term $\Omega \hat{J}_{rg}$ only 'feels' the atoms in states $|g\rangle$ and $|r\rangle$. Therefore, to first order in Ω it effectively gives a collective excitation from $N_g = N/2 - m$ atoms in state $|g\rangle$ to a single symmetric excitation at state $|r\rangle$ (the state $|m, 1\rangle$), and so experiences the known enhancement of square root of the atom number, which here is N_g .
- Decay $\gamma_r (N/2 + m + 1)$: The collective decay term $\gamma_r \mathcal{D}_{\hat{j}_{er}}[\hat{R}]$ only 'feels' the atoms in states $|e\rangle$ and $|r\rangle$. So, here it describes the decay from a singly excited atom at $|r\rangle$ to $N_e = N/2 + m$ atoms at $|e\rangle$. This decay is symmetric, i.e. does not distinguish between atoms, since the original states $|m, 0\rangle$ and $|m+1, 0\rangle$ are symmetric (Dicke states). This means we effectively have a decay of a symmetric system of $N_e + 1$ atoms in total, which is commonly known to exhibit the collective enhancement of the factor of the number of atoms, hence yielding $\gamma_r (N_e + 1)$.
- Decay $\gamma_m = \gamma [N/2 (N/2 + 1) - m(m + 1)]$: The usual decay between the two Dicke states $|m+1\rangle$ and $|m\rangle$ in the $\{g, e\}$ subspace. A similar decay γ_{m-1} from $|m\rangle$ to the state $|m-1\rangle$ outside of this diagram also exists.

We now turn to consider the adiabatic elimination of the state $|m, 1\rangle$ which includes the r -manifold. Assuming times t much shorter than the 'free' dynamics of the $\{g, e\}$ subspace (i.e. those governed by the term $\gamma \mathcal{D}_{\hat{j}_{ge}}[\hat{R}]$ that does not involve the states $|r\rangle$, at rate $\sim \gamma_m$), and solving for times much longer than $1/\delta$, the steady state population of the state $|m, 1\rangle$ (within our coarse-graining time $1/\delta \ll t \ll 1/\gamma_m$), has the usual Lorentzian-like form:

$$p_{m,1} \approx \frac{N_g \Omega^2}{\delta^2 + \gamma_r^2 (N_e + 1)^2 / 4}. \quad (\text{B15})$$

Then, since this population decays at rate $(N_e + 1) \gamma_r$ to $|m, 0\rangle$, the total rate of the incoherent process from $|m, 0\rangle$

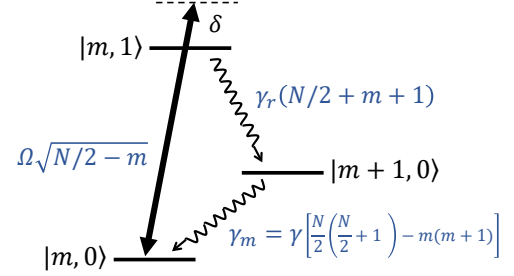


FIG. 5. Relevant level scheme considered in Appendix B 3.

to $|m+1, 0\rangle$ is given by the product of this population and its decay, yielding $w_m = p_{m,1} (N_e + 1) \gamma_r$.

This incoherent process is then described by the jump operator $\sqrt{w_m} |m+1\rangle \langle m|$, which is only within the $\{g, e\}$ subspace. Summing over the incoherent processes from different states $|m\rangle$, we then obtain the total jump operator $\sum_m |m+1\rangle \langle m| \sqrt{w_m}$. As we see below, the latter can take an appealing form if we make the denominator of $p_{m,1}$ independent of m , i.e. assuming $\delta \gg (N/2 + m + 1) \gamma_r$. Taken together with the separation of timescales we already assumed in the adiabatic elimination (coarse graining time), we have the condition: $\delta \gg (N/2 + m + 1) \gamma_r, \gamma_m, \Omega\sqrt{N/2 - m}$ which to be satisfied for all states m requires:

$$\delta \gg \sqrt{N} \Omega, N \gamma_r, N^2 \gamma, \quad (\text{B16})$$

as stated in the main text and in agreement with the results of subsection A above. With this, we can take $p_{m+1} \approx (N/2 - m) \Omega^2 / \delta^2$ in Eq. (B15) and obtain the total jump operator

$$\sum_m |m+1\rangle \langle m| \sqrt{w_m} \approx \sqrt{\gamma_r} \frac{\Omega}{\delta} \hat{J}_+ \equiv \sqrt{w} \hat{J}_+. \quad (\text{B17})$$

This indeed yields the optical pumping term $w \mathcal{D}_{\hat{j}_+}[\hat{R}]$ in Eq. (1) of the main text with $w = \gamma_r (\Omega/\delta)^2$.

Appendix C: Analytical calculation of steady state and numerical validation of its uniqueness

In Eq. (3) of the text we stated that the system has a unique steady state of the form:

$$\hat{\rho}_\beta \propto e^{-\beta \hat{J}_z}, \quad (\text{C1})$$

with $\beta = -\ln(w/\gamma)$. We show that this is a solution by direct substitution. To this end we use the identities:

$$e^{\beta \hat{J}_z} \hat{J}_- e^{-\beta \hat{J}_z} = e^{-\beta} \hat{J}_-, \quad e^{\beta \hat{J}_z} \hat{J}_+ e^{-\beta \hat{J}_z} = e^{\beta} \hat{J}_+, \quad (\text{C2})$$

$$\left[\hat{J}_+ \hat{J}_-, e^{-\beta \hat{J}_z} \right] = \left[\hat{J}_- \hat{J}_+, e^{-\beta \hat{J}_z} \right] = 0.$$

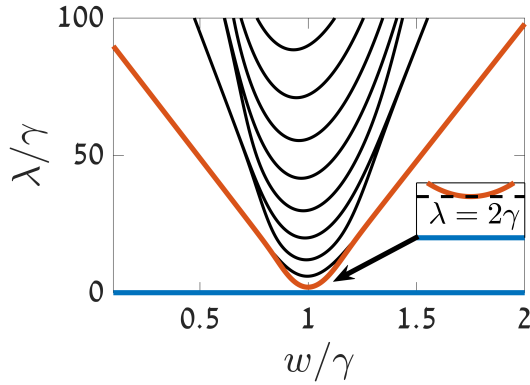


FIG. 6. Lindbladian spectrum of \mathcal{L} in the $\text{Diag}^{(0)}$ sector, for $N = 100$. The blue curve represents the zero mode, the red curve represents the Lindbladian gap and the black curves show the higher dissipative modes. Inside the closeup of the transition point we see a minimal gap of $\lambda = 2\gamma$.

Moving on to the calculation:

$$\begin{aligned}
\dot{\hat{\rho}}_\beta &\propto \gamma \mathcal{D}_{\hat{J}_-} [\hat{\rho}_\beta] + w \mathcal{D}_{\hat{J}_+} [\hat{\rho}_\beta] \\
&= \gamma \left(\hat{J}_- e^{-\beta \hat{J}_z} \hat{J}_+ - \frac{1}{2} \left\{ \hat{J}_+ \hat{J}_-, e^{-\beta \hat{J}_z} \right\} \right) \\
&+ \gamma e^{-\beta} \left(\hat{J}_+ e^{-\beta \hat{J}_z} \hat{J}_- - \frac{1}{2} \left\{ \hat{J}_- \hat{J}_+, e^{-\beta \hat{J}_z} \right\} \right) \\
&= \gamma e^{-\beta \hat{J}_z} \left(\left(e^{\beta \hat{J}_z} \hat{J}_- e^{-\beta \hat{J}_z} \right) \hat{J}_+ - \hat{J}_+ \hat{J}_- \right) \\
&+ \gamma e^{-\beta} \cdot e^{-\beta \hat{J}_z} \left(\left(e^{\beta \hat{J}_z} \hat{J}_+ e^{-\beta \hat{J}_z} \right) \hat{J}_- - \hat{J}_- \hat{J}_+ \right) \\
&= \gamma e^{-\beta \hat{J}_z} \left(e^{-\beta} \hat{J}_- \hat{J}_+ - \hat{J}_+ \hat{J}_- \right) \\
&+ \gamma e^{-\beta \hat{J}_z} \left(e^{-\beta} \cdot e^{\beta} \hat{J}_+ \hat{J}_- - e^{-\beta} \hat{J}_- \hat{J}_+ \right) \\
&= 0.
\end{aligned} \tag{C3}$$

So this is indeed a steady state. To be sure of its uniqueness, consider first the following decomposition of the space of density matrices into off-diagonals:

$$\begin{aligned}
\hat{\rho} &= \sum_{q=-N}^N \hat{\rho}^{(q)}, \quad \hat{\rho}^{(q)} \in \text{Diag}^{(q)} \\
&= \begin{cases} \text{span} \{ |m\rangle \langle m+q| \}_{m=-N/2}^{N/2-q} & q \geq 0 \\ \text{Diag}^{(-q)\dagger} & q < 0 \end{cases}.
\end{aligned} \tag{C4}$$

One can be easily convinced that the evolution operator $\mathcal{L} \equiv \gamma \mathcal{D}_{\hat{J}_-} + w \mathcal{D}_{\hat{J}_+}$ maps elements of $\text{Diag}^{(q)}$ to elements of $\text{Diag}^{(q)}$, and thus decomposes as a direct sum over these spaces. This means that the modes of the system can be found by diagonalizing \mathcal{L} over each subspace individually, which is easily done on a computer. In Fig. 6 the resulting spectrum for the diagonal subspace $\text{Diag}^{(0)}$ is shown, with only one zero eigenvalue (representing the steady state) and with the smallest nonzero eigenvalue having a gap of $\lambda = 2\gamma$. The spectrum in all other subspaces is similarly gapped, with the smallest

gap appearing in $\text{Diag}^{(\pm 1)}$ and having a value of $\lambda = \gamma$. This ensures us that the system has only one steady state, and that any perturbation decays at most after a time $\tau \sim 1/\gamma$.

Appendix D: Cramér–Rao bound for the sensitivity

In the text’s Eq. (5) we gave an estimate of the steady state sensitivity to changes in the pumping rate, finding it to be of $O(1/N)$. We now make this more exact by using the Cramér–Rao bound with respect to the estimated parameter $\beta = -\ln(w/\gamma)$. To this end we note that the distribution of \hat{J}_z values is given by

$$p_m(\beta) = \langle m | \hat{\rho}_\beta | m \rangle = \frac{1}{Z(\beta)} e^{-\beta m}, \tag{D1}$$

$$Z(\beta) = \frac{\sinh\left(\frac{N+1}{2}\beta\right)}{\sinh\left(\frac{1}{2}\beta\right)}. \tag{D2}$$

Since the state is diagonal in this basis for all β , we know that the quantum Fisher with respect to β is the same as the classical Fisher information [65], and we can compute it as

$$\begin{aligned}
I_\beta &= \sum_m p_m(\beta) (\partial_\beta \ln p_m(\beta))^2 \\
&= \sum_m p_m(\beta) (m + \partial_\beta \ln Z(\beta))^2 \\
&= \text{tr} \left(\hat{\rho}_\beta \left(\hat{J}_z - \langle \hat{J}_z \rangle \right)^2 \right) \\
&= \text{Var}[\hat{J}_z].
\end{aligned} \tag{D3}$$

We now have a formal bound on the possible precision with which we can estimate β :

$$\delta\beta \geq \frac{1}{\sqrt{I_\beta}} = \frac{1}{\sqrt{\text{Var}[\hat{J}_z]}}. \tag{D4}$$

Lastly, we note that at the transition the variance as presented in Eq. (D3) achieves the value

$$\text{Var}[\hat{J}_z]_{|\beta=0} = -\partial_\beta \langle \hat{J}_z \rangle = \frac{N^2}{12}, \tag{D5}$$

so inputting this result (and replacing $\delta\beta = \frac{\delta w}{w}$), we get the bound

$$\frac{\delta w}{w} \geq \frac{\sqrt{12}}{N}, \tag{D6}$$

which is found to be saturated by the metrology scheme presented in the main text.

Appendix E: Calculation of the relaxation rate λ by numerical diagonalization and by cumulant methods

Since calculation of the mean inversion $\langle \hat{J}_z(t) \rangle = \text{tr}(\hat{J}_z \hat{\rho}(t))$ requires only diagonal matrix elements

(which as stated in Appendix C evolve independently in the $\text{Diag}^{(0)}$ subspace), the spectrum shown in Fig. 6 contains all rates governing the evolution of the mean, and in particular the lowest nonzero eigenvalue $\lambda(w)$ represents the exact asymptotic rate at which $\langle \hat{J}_z(t) \rangle$ decays. We contrast this with an approximate analytical expression which we obtain by analyzing the two time correlation C_{zz} given by

$$C_{zz}(\tau) \equiv \langle \hat{J}_z(t+\tau) \hat{J}_z(t) \rangle - \langle \hat{J}_z(t+\tau) \rangle \langle \hat{J}_z(t) \rangle. \quad (\text{E1})$$

At long times these correlations decay at a rate $C_{zz}(\tau) \sim e^{-\lambda(w)\tau}$, which can be approximately calculated by writing the rate equation for C_{zz} obtained from the master equation in terms of higher order correlations

$$\begin{aligned} \partial_\tau C_{zz}(\tau) &= (w - \gamma) \langle \hat{J}_z^2(t+\tau) \hat{J}_z(t) \rangle \\ &\quad - (w - \gamma) \langle \hat{J}_z^2(t+\tau) \rangle \langle \hat{J}_z(t) \rangle \\ &\quad - (w + \gamma) C_{zz}(\tau), \end{aligned} \quad (\text{E2})$$

and then breaking these correlations into lower order ones by neglecting third order cumulants [67]

$$\begin{aligned} \langle \hat{J}_z^2(t+\tau) \hat{J}_z(t) \rangle &\approx 2 \langle \hat{J}_z(t+\tau) \rangle C_{zz}(\tau) \\ &\quad + \langle \hat{J}_z^2(t+\tau) \rangle \langle \hat{J}_z(t) \rangle. \end{aligned} \quad (\text{E3})$$

In this way we reach an expression for the decay rate

$$\partial_\tau C_{zz} = -2 \left(\frac{w+\gamma}{2} + (w - \gamma) \langle \hat{J}_z \rangle \right) C_{zz} \rightarrow \quad (\text{E4})$$

$$\lambda(w) = w + \gamma + 2(w - \gamma) \langle \hat{J}_z \rangle(w), \quad (\text{E5})$$

where the mean inversion $\langle \hat{J}_z \rangle$ can be calculated directly by using the partition function in Eq. (D2):

$$\begin{aligned} \langle \hat{J}_z \rangle &= -\partial_\beta \ln Z(\beta) |_{\beta=-\ln(w/\gamma)} \\ &= \frac{N+1}{2} \frac{(w/\gamma)^{N+1} + 1}{(w/\gamma)^{N+1} - 1} - \frac{1}{2} \frac{w/\gamma + 1}{w/\gamma - 1}, \end{aligned} \quad (\text{E6})$$

and in the limit $N \gg 1$, $|w/\gamma - 1| \ll 1$ is given by

$$\langle \hat{J}_z \rangle \rightarrow \frac{N/2}{\tanh(N(w/\gamma - 1)/2)} - \frac{1}{w/\gamma - 1}. \quad (\text{E7})$$

This expression for $\lambda(w)$ was compared in Fig. 2 of the paper against the lowest nonzero eigenvalue appearing in Fig. 6. While the numerical and analytical curves approximately agree, we note that there is a discrepancy between them of order γ . As $N \rightarrow \infty$ this discrepancy persists, but the scale of λ away from the transition grows with N so as to make this error negligible. At the transition this error cannot be said to be negligible, because the relaxation rate approaches a minimum value of $\lambda = 2\gamma$. However, both curves agree on this minimum value such that the asymptotic expression in Eq. (E5) is correct.

Appendix F: Hysteresis width power law

In the paper we derived a scaling law for the hysteresis width Δw_H as a function of the scanning rate $r = N\dot{w}/2\gamma$, as presented in Eq. (8) of the paper. That we compared to a dynamical simulation of the master equation in Eq. (B13), where we varied the pumping at a rate r and measured the width of the resulting hysteresis. The results, shown in Fig. 4 of the paper, indicated a scaling exponent of $\eta \approx 0.6$ instead of the expected $\eta = 1/2$ power law.

To explain this discrepancy, we remember a fundamental assumption taken while estimating the hysteresis width, namely that the $\langle \hat{J}_z \rangle$ dynamics are characterized by a single decay rate $\lambda(w)$, as given in Eq. (E5). Looking back at figure Fig. 6, we see that the real situation is more complicated. There are multiple eigenvalues characterizing the dynamics, and there is no clear separation between the first dissipative mode (equal to $\lambda(w)$) and the higher modes. This means that for rates $r \gg \gamma$ there is no well defined single rate at which the system decays, and so our calculation of the adiabatic boundary (as depicted in Fig. 3 of the paper) is "perturbed" by the influence of higher modes. This explains the slightly deviated exponent 0.6.

-
- [1] F. Minganti, A. Biella, N. Bartolo, and C. Ciuti, Spectral theory of liouvillians for dissipative phase transitions, *Physical Review A* **98**, 042118 (2018).
- [2] T. E. Lee, H. Haefner, and M. C. Cross, Collective quantum jumps of rydberg atoms, *Physical review letters* **108**, 023602 (2012).
- [3] J. Marino and S. Diehl, Quantum dynamical field theory for nonequilibrium phase transitions in driven open systems, *Physical Review B* **94**, 085150 (2016).
- [4] B. Zhu, J. Marino, N. Y. Yao, M. D. Lukin, and E. A. Demler, Dicke time crystals in driven-dissipative quantum many-body systems, *New Journal of Physics* **21**, 073028 (2019).
- [5] M. Marcuzzi, E. Levi, S. Diehl, J. P. Garrahan, and I. Lesanovsky, Universal nonequilibrium properties of dissipative rydberg gases, *Physical review letters* **113**, 210401 (2014).
- [6] C. Sánchez Muñoz, B. Buča, J. Tindall, A. González-Tudela, D. Jaksch, and D. Porras, Symmetries and conservation laws in quantum trajectories: Dissipative freezing, *Physical Review A* **100**, 042113 (2019).
- [7] C.-K. Chan, T. E. Lee, and S. Gopalakrishnan, Limit-cycle phase in driven-dissipative spin systems, *Physical Review A* **91**, 051601 (2015).

- [8] M. Hoening, W. Abdussalam, M. Fleischhauer, and T. Pohl, Antiferromagnetic long-range order in dissipative rydberg lattices, *Physical Review A* **90**, 021603 (2014).
- [9] H. Weimer, Variational principle for steady states of dissipative quantum many-body systems, *Physical review letters* **114**, 040402 (2015).
- [10] R. M. Wilson, K. W. Mahmud, A. Hu, A. V. Gorshkov, M. Hafezi, and M. Foss-Feig, Collective phases of strongly interacting cavity photons, *Physical Review A* **94**, 033801 (2016).
- [11] P. Comaron, G. Dagvadorj, A. Zamora, I. Carusotto, N. P. Proukakis, and M. H. Szymańska, Dynamical critical exponents in driven-dissipative quantum systems, *Physical review letters* **121**, 095302 (2018).
- [12] F. Vicentini, F. Minganti, R. Rota, G. Orso, and C. Ciuti, Critical slowing down in driven-dissipative bose-hubbard lattices, *Physical Review A* **97**, 013853 (2018).
- [13] E. M. Kessler, G. Giedke, A. Imamoglu, S. F. Yelin, M. D. Lukin, and J. I. Cirac, Dissipative phase transition in a central spin system, *Physical Review A* **86**, 012116 (2012).
- [14] L. M. Sieberer, S. D. Huber, E. Altman, and S. Diehl, Dynamical critical phenomena in driven-dissipative systems, *Physical review letters* **110**, 195301 (2013).
- [15] T. E. Lee, C.-K. Chan, and S. F. Yelin, Dissipative phase transitions: Independent versus collective decay and spin squeezing, *Physical Review A* **90**, 052109 (2014).
- [16] D. Goncalves, L. Bombieri, G. Ferioli, S. Pancaldi, I. Ferrier-Barbut, A. Browaeys, E. Shahmoon, and D. E. Chang, Driven-dissipative phase separation in free-space atomic ensembles, *arXiv preprint arXiv:2403.15237* (2024).
- [17] S. Diehl, A. Tomadin, A. Micheli, R. Fazio, and P. Zoller, Dynamical phase transitions and instabilities in open atomic many-body systems, *Physical review letters* **105**, 015702 (2010).
- [18] B. Kraus, H. P. Büchler, S. Diehl, A. Kantian, A. Micheli, and P. Zoller, Preparation of entangled states by quantum markov processes, *Physical Review A* **78**, 042307 (2008).
- [19] S. Diehl, A. Micheli, A. Kantian, B. Kraus, H. P. Büchler, and P. Zoller, Quantum states and phases in driven open quantum systems with cold atoms, *Nature Physics* **4**, 878 (2008).
- [20] H. Weimer, M. Müller, I. Lesanovsky, P. Zoller, and H. P. Büchler, A rydberg quantum simulator, *Nature Physics* **6**, 382 (2010).
- [21] Y. Lin, J. P. Gaebler, F. Reiter, T. R. Tan, R. Bowler, A. S. Sørensen, D. Leibfried, and D. J. Wineland, Dissipative production of a maximally entangled steady state of two quantum bits, *Nature* **504**, 415 (2013).
- [22] M. J. Kastoryano, F. Reiter, and A. S. Sørensen, Dissipative preparation of entanglement in optical cavities, *Physical review letters* **106**, 090502 (2011).
- [23] F. Reiter and A. S. Sorensen, Effective operator formalism for open quantum systems, *Physical Review A* **85**, 032111 (2012).
- [24] F. Verstraete, M. M. Wolf, and J. Ignacio Cirac, Quantum computation and quantum-state engineering driven by dissipation, *Nature physics* **5**, 633 (2009).
- [25] A. Beige, D. Braun, B. Tregenna, and P. L. Knight, Quantum computing using dissipation to remain in a decoherence-free subspace, *Physical review letters* **85**, 1762 (2000).
- [26] B. Rost, L. Del Re, N. Earnest, A. F. Kemper, B. Jones, and J. K. Freericks, Demonstrating robust simulation of driven-dissipative problems on near-term quantum computers, *arXiv preprint arXiv:2108.01183* (2021).
- [27] M. Koppenhöfer, P. Groszkowski, H.-K. Lau, and A. A. Clerk, Dissipative superradiant spin amplifier for enhanced quantum sensing, *PRX Quantum* **3**, 030330 (2022).
- [28] M. Müller, K. Hammerer, Y. L. Zhou, C. F. Roos, and P. Zoller, Simulating open quantum systems: from many-body interactions to stabilizer pumping, *New Journal of Physics* **13**, 085007 (2011).
- [29] D.-S. Ding, Z.-K. Liu, B.-S. Shi, G.-C. Guo, K. Molmer, and C. S. Adams, Enhanced metrology at the critical point of a many-body rydberg atomic system, *Nature Physics* **18**, 1447 (2022).
- [30] S. Gammelmark and K. Molmer, Phase transitions and heisenberg limited metrology in an ising chain interacting with a single-mode cavity field, *New Journal of Physics* **13**, 053035 (2011).
- [31] C. S. Adams, J. D. Pritchard, and J. P. Shaffer, Rydberg atom quantum technologies, *Journal of Physics B: Atomic, Molecular and Optical Physics* **53**, 012002 (2019).
- [32] V. P. Pavlov, D. Porras, and P. A. Ivanov, Quantum metrology with critical driven-dissipative collective spin system, *Physica Scripta* **98**, 095103 (2023).
- [33] S. Fernández-Lorenzo and D. Porras, Quantum sensing close to a dissipative phase transition: Symmetry breaking and criticality as metrological resources, *Physical Review A* **96**, 013817 (2017).
- [34] K. Stannigel, P. Rabl, and P. Zoller, Driven-dissipative preparation of entangled states in cascaded quantum-optical networks, *New Journal of Physics* **14**, 063014 (2012).
- [35] M. M. Rams, P. Sierant, O. Dutta, P. Horodecki, and J. Zakrzewski, At the limits of criticality-based quantum metrology: apparent super-heisenberg scaling revisited, *Physical Review X* **8**, 021022 (2018).
- [36] K. Gietka, F. Metz, T. Keller, and J. Li, Adiabatic critical quantum metrology cannot reach the heisenberg limit even when shortcuts to adiabaticity are applied, *Quantum* **5**, 489 (2021).
- [37] L. Garbe, M. Bina, A. Keller, M. G. A. Paris, and S. Felicetti, Critical quantum metrology with a finite-component quantum phase transition, *Physical review letters* **124**, 120504 (2020).
- [38] L. Henriët, J. S. Douglas, D. E. Chang, and A. Albrecht, Critical open-system dynamics in a one-dimensional optical-lattice clock, *Physical Review A* **99**, 023802 (2019).
- [39] R. H. Dicke, Coherence in spontaneous radiation processes, *Physical review* **93**, 99 (1954).
- [40] M. Gross and S. Haroche, Superradiance: An essay on the theory of collective spontaneous emission, *Physics reports* **93**, 301 (1982).
- [41] P. Kirton, M. M. Roses, J. Keeling, and E. G. Dalla Torre, Introduction to the dicke model: From equilibrium to nonequilibrium, and vice versa, *Advanced Quantum Technologies* **2**, 1800043 (2019).
- [42] S. J. Masson and A. Asenjo-Garcia, Universality of dicke superradiance in arrays of quantum emitters, *Nature Communications* **13**, 2285 (2022).

- [43] P. D. Drummond and H. J. Carmichael, Volterra cycles and the cooperative fluorescence critical point, *Optics Communications* **27**, 160 (1978).
- [44] H. J. Carmichael, Analytical and numerical results for the steady state in cooperative resonance fluorescence, *Journal of Physics B: Atomic and Molecular Physics* **13**, 3551 (1980).
- [45] D. Barberena, R. J. Lewis-Swan, J. K. Thompson, and A. M. Rey, Driven-dissipative quantum dynamics in ultra-long-lived dipoles in an optical cavity, *Physical Review A* **99**, 053411 (2019).
- [46] K. Tucker, D. Barberena, R. J. Lewis-Swan, J. K. Thompson, J. G. Restrepo, and A. M. Rey, Facilitating spin squeezing generated by collective dynamics with single-particle decoherence, *Physical Review A* **102**, 051701 (2020).
- [47] A. González-Tudela and D. Porras, Mesoscopic entanglement induced by spontaneous emission in solid-state quantum optics, *Physical review letters* **110**, 080502 (2013).
- [48] C. Qu and A. M. Rey, Spin squeezing and many-body dipolar dynamics in optical lattice clocks, *Physical Review A* **100**, 041602 (2019).
- [49] O. Somech and E. Shahmoon, Quantum entangled states of a classically radiating macroscopic spin, *PRX Quantum* **5**, 010349 (2024).
- [50] O. Somech, Y. Shimshi, and E. Shahmoon, Heisenberg-langevin approach to driven superradiance, *Physical Review A* **108**, 023725 (2023).
- [51] G. Ferioli, A. Glicenstein, I. Ferrier-Barbut, and A. Browaeys, A non-equilibrium superradiant phase transition in free space, *Nature Physics*, 1 (2023).
- [52] M. A. Norcia, M. N. Winchester, J. R. K. Cline, and J. K. Thompson, Superradiance on the millihertz linewidth strontium clock transition, *Science advances* **2**, e1601231 (2016).
- [53] M. A. Norcia and J. K. Thompson, Cold-strontium laser in the superradiant crossover regime, *Physical Review X* **6**, 011025 (2016).
- [54] T. Maier, S. Kraemer, L. Ostermann, and H. Ritsch, A superradiant clock laser on a magic wavelength optical lattice, *Optics express* **22**, 13269 (2014).
- [55] J. G. Bohnet, Z. Chen, J. M. Weiner, D. Meiser, M. J. Holland, and J. K. Thompson, A steady-state superradiant laser with less than one intracavity photon, *Nature* **484**, 78 (2012).
- [56] D. Meiser, J. Ye, D. R. Carlson, and M. J. Holland, Prospects for a millihertz-linewidth laser, *Physical review letters* **102**, 163601 (2009).
- [57] D. Meiser and M. J. Holland, Intensity fluctuations in steady-state superradiance, *Physical Review A* **81**, 063827 (2010).
- [58] D. Meiser and M. J. Holland, Steady-state superradiance with alkaline-earth-metal atoms, *Physical Review A* **81**, 033847 (2010).
- [59] D. A. Tieri, M. Xu, D. Meiser, J. Cooper, and M. J. Holland, Theory of the crossover from lasing to steady state superradiance, arXiv preprint arXiv:1702.04830 (2017).
- [60] L. Pezze and A. Smerzi, Entanglement, nonlinear dynamics, and the heisenberg limit, *Physical review letters* **102**, 100401 (2009).
- [61] D. J. Wineland, J. J. Bollinger, W. M. Itano, F. L. Moore, and D. J. Heinzen, Spin squeezing and reduced quantum noise in spectroscopy, *Physical Review A* **46**, R6797 (1992).
- [62] D. J. Wineland, J. J. Bollinger, W. M. Itano, and D. J. Heinzen, Squeezed atomic states and projection noise in spectroscopy, *Physical Review A* **50**, 67 (1994).
- [63] K. Binder and D. P. Landau, Finite-size scaling at first-order phase transitions, *Physical Review B* **30**, 1477 (1984).
- [64] N. Berglund, *Adiabatic dynamical systems and hysteresis*, Tech. Rep. (1998).
- [65] K. C. Tan and H. Jeong, Nonclassical light and metrological power: An introductory review, *AVS Quantum Science* **1** (2019).
- [66] S. Swain, Master equation derivation of quantum regression theorem, *Journal of Physics A: Mathematical and General* **14**, 2577 (1981).
- [67] R. Kubo, Generalized cumulant expansion method, *Journal of the Physical Society of Japan* **17**, 1100 (1962).
- [68] I. D. Leroux, M. H. Schleier-Smith, and V. Vuletić, Implementation of cavity squeezing of a collective atomic spin, *Physical Review Letters* **104**, 073602 (2010).
- [69] M. H. Schleier-Smith, I. D. Leroux, and V. Vuletić, Squeezing the collective spin of a dilute atomic ensemble by cavity feedback, *Physical Review A—Atomic, Molecular, and Optical Physics* **81**, 021804 (2010).
- [70] Z. Yan, J. Ho, Y.-H. Lu, S. J. Masson, A. Asenjo-Garcia, and D. M. Stamper-Kurn, Superradiant and subradiant cavity scattering by atom arrays, *Physical Review Letters* **131**, 253603 (2023).